REVIEW



Check for updates

Probing interfacial electrochemistry by in situ atomic force microscope for battery characterization

Manman Wang¹ | Zhibo Song² | Jinxin Bi¹ | Huanxin Li³ | Ming Xu¹ | Yi Gong¹ | Yundong Zhou⁴ | Yunlong Zhao^{1,4} | Kai Yang¹

Correspondence

Yundong Zhou, National Physical Laboratory, Teddington, Middlesex TW11 0LW, UK.

Email: yundong.zhou@npl.co.uk

Yunlong Zhao and Kai Yang, Department of Electrical and Electronic Engineering, Advanced Technology Institute, University of Surrey, Guildford, Surrey GU2 7XH, UK.

Email: yunlong.zhao@surrey.ac.uk and kai.yang@surrey.ac.uk

EPSRC New Investigator Award,

Funding information

Grant/Award Number: EP/V002260/1; Faraday Institution—Battery Study and Seed Research Project, Grant/Award Number: FIRG052; Metrology and Standards for the Battery Value Chain of the National Measurement System of the UK Department of Business, Energy and Industrial Strategy; University of Surrey Vice-Chancellor's Studentship

Abstract

Lithium-ion batteries (LIBs) have been widely used in electric vehicles and energy storage industries. An understanding of the reaction processes and degradation mechanism in LIBs is crucial for optimizing their performance. In situ atomic force microscopy (AFM) as a surface-sensitive tool has been applied in the real-time monitoring of the interfacial processes within lithium batteries. Here, we reviewed the recent progress of the application of in situ AFM for battery characterizations, including LIBs, lithium-sulfur batteries, and lithium-oxygen batteries. We summarized advances in the in situ AFM for recording electrode/electrolyte interface, mechanical properties, morphological changes, and surface evolution. Future directions of in situ AFM for the development of lithium batteries were also discussed in this review.

KEYWORDS

electrode/electrolyte interface, in situ atomic force microscopy, lithium batteries, mechanical properties, morphological and surface evolution

1 | INTRODUCTION

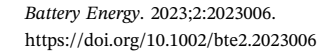
Lithium-ion batteries (LIBs) have attracted continuous attention since their inception and have been widely used in electronic devices, electric vehicles, energy storage devices, and beyond.^{1–7} Due to the limited theoretical capacity of LIBs, new lithium battery

systems with high theoretical capacity (such as Li–air batteries^{8–11} and Li–sulfur batteries^{12–15}) have also been extensively studied to meet the increasing energy demand. To develop high-performance batteries with high energy and power density, high Coulombic efficiency, long cycle life, and improved safety, a multiscale and multidimensional understanding of the

Manman Wang and Zhibo Song contributed equally to this study.

This is an open access article under the terms of the Creative Commons Attribution License, which permits use, distribution and reproduction in any medium, provided the original work is properly cited.

© 2023 The Authors. Battery Energy published by Xijing University and John Wiley & Sons Australia, Ltd.



¹Department of Electrical and Electronic Engineering, Advanced Technology Institute, University of Surrey, Guildford, Surrey, UK

²School of Advanced Materials, Peking University Shenzhen Graduate School, Shenzhen, China

³Physical & Theoretical Chemistry Laboratory, Department of Chemistry, University of Oxford, Oxford, UK

⁴National Physical Laboratory, Teddington, Middlesex, UK

27681696, 2023, 6, Downloaded from https://onlinelibrary.wiley.com/doi/10.1002/bte2.2023006 by Test, Wiley Online Library on [13/99/2024]. See the Terms and Conditions (https://onlinelibrary.wiley.com/rems-a-d-conditions) on Wiley Online Library for rules of use; OA articles are governed by the applicable Cerative Commons Licenses

battery materials, interfaces, and processes is of great significance.

The performance of the lithium batteries depends on a variety of interfacial processes and reactions within them, including the morphological and volume changes of electrode caused by ion intercalation/deintercalation, the formation of solid–electrolyte interphase (SEI) and cathode–electrolyte interphase (CEI) initiated by electrolyte decomposition, and the dendrite growth induced by uneven lithium plating and stripping. ^{16–19} Therefore, combining advanced in situ characterization techniques to observe the interfacial processes and reactions within LIBs in real time could contribute to better investigation of the battery operation and degradation mechanism,

thus providing directions for optimizing battery performance.

In the past decades, various advanced techniques have been applied to investigate the material properties of LIBs and interfacial processes. Among various in situ characterization techniques (X-ray-based microscopes, electron microscopes, scanning probe microscopes [SPMs], etc.), in situ atomic force microscopy (AFM) is a valuable technique for battery research due to its high spatial resolution, ability to directly image surface morphology and mechanical properties, and versatility in sample preparation and operating conditions. In situ AFM can provide high-resolution morphological, mechanical, and electrical information over a large length scale (nanometers to tens of micrometers) and

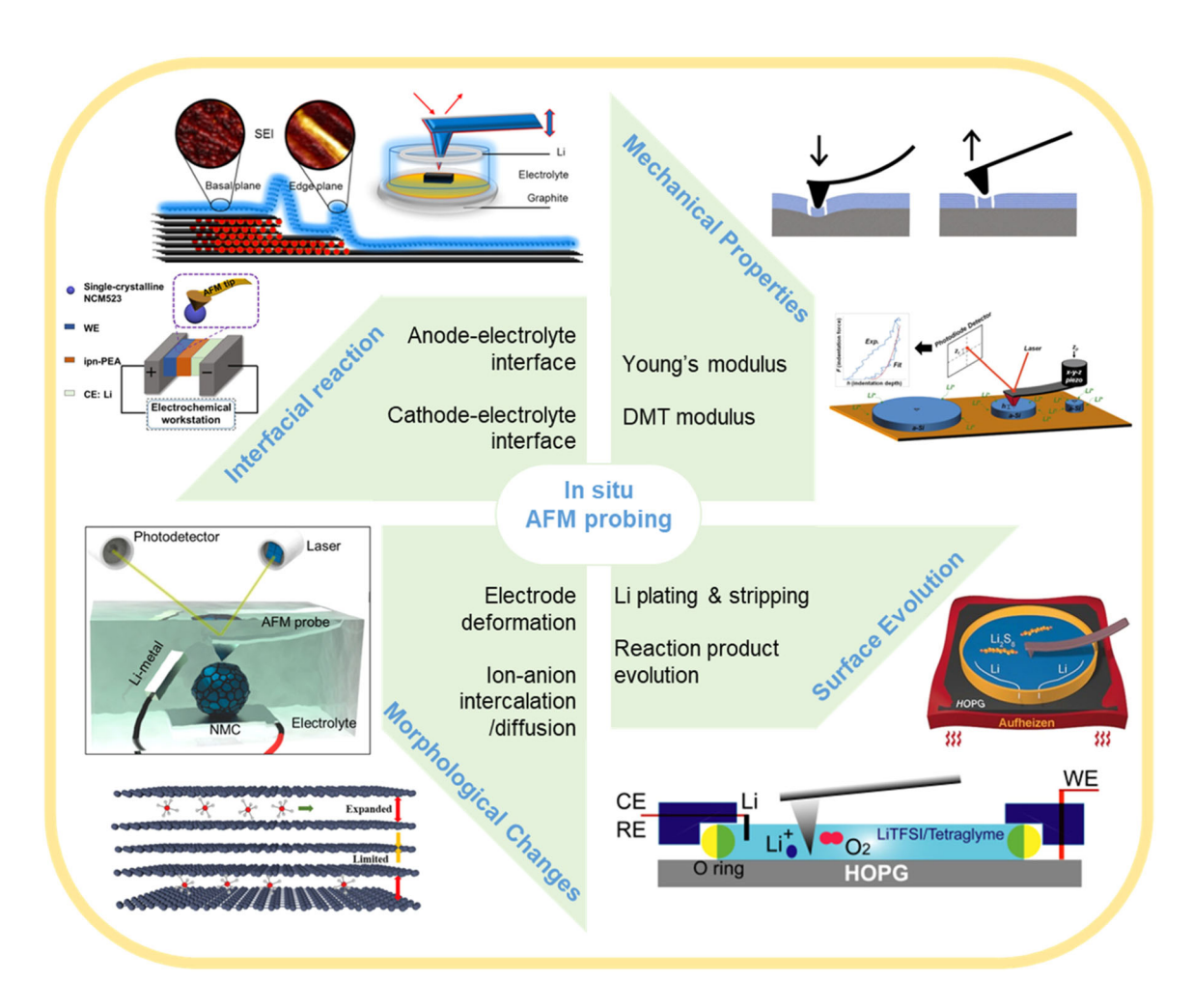


FIGURE 1 Overview of the applications of in situ atomic force microscopy (AFM) for lithium batteries. Anode–electrolyte interface characterization image. Reproduced with permissions.²⁶ Copyright 2020, American Chemical Society. Cathode–electrolyte interface characterization image. Reproduced with permission.²⁷ Copyright 2022, Wiley-VCH GmbH. AFM indentation image. Reproduced with permission.²⁸ Copyright 2020, Elsevier Inc. Silicon electrode image. Reproduced with permission.²⁹ Copyright 2014, Elsevier B.V. Li–S battery characterization image. Reproduced with permission.³⁰ Copyright 2017, Wiley-VCH GmbH. Li–O₂ battery characterization image. Reproduced with permission.³¹ Copyright 2013, American Chemical Society. NMC deformation characterization image. Reproduced with permission.³² Copyright 2020, Elsevier Ltd. Anion intercalation characterization image. Reproduced with permission.³³ Copyright 2020, Tsinghua University Press and Springer-Verlag GmbH Germany, part of Springer Nature. CE, counter electrode; DMT, Derjaguin–Muller–Toporov; HOPG, highly oriented pyrolytic graphite; PES, 1% prop-1-ene-1,3-sultone; RE, reference electrode; WE, working electrode.

high adaptation in different atmospheres, enabling the possibility to monitor the interfacial changes in nanoscale resolution and in real time. 20-22 Directly imaging of surface morphology and topography during electrochemical reactions can also be achieved by in situ AFM, providing insights into phenomena such as surface roughening, dendrite growth, and phase transformation. In addition, in situ AFM can be used to measure mechanical properties such as adhesion and stiffness, which are important for understanding the mechanical evolution of electrodes. Another advantage of in situ AFM is its versatility in terms of sample preparation and operating conditions. Unlike Xray diffraction (XRD) or scanning electron microscope, which often require specialized sample preparation and vacuum environments, AFM can be used with a wide range of electrode materials and electrolytes. Moreover, AFM can operate in a variety of gas atmospheres (ambient air, inert gas, or vacuum) as well as in liquid environments. 23-25 enabling studies of various electrochemical reactions and interfaces.

In this review, we briefly review the applications of the in situ AFM in LIBs and Li-sulfur batteries, as well as in Li-air batteries. We mainly discuss the in situ AFM techniques for investigating electrode-electrolyte interfaces, mechanical properties, morphological changes, and surface evolution (Figure 1). We believe that the in situ AFM would make great contributions to the in-depth understanding of the operation, degradation, and failure mechanism of batteries, promoting the development of lithium batteries.

ELECTRODE-ELECTROLYTE **INTERFACES**

The properties of the electrode–electrolyte interface play a key role in determining lithium battery performance. 34,35 For example, the decomposition of the electrolyte leads to the generation of SEI on the anode and CEI on the cathode, whose physical and chemical properties (including morphology, thickness, compactness, and composition) affect the cyclability, capacity, and safety of the battery. The in situ AFM provides a direct visualization for observing the interfacial processes at a high resolution and in real time, contributing to the analysis of the structure and properties of SEI and CEI.

Anode-electrolyte interface 2.1

SEI is an ionically conductive but electronically insulating layer, which is formed by the reductive decomposition of the electrolyte (lithium salt, solvent, and additives) during the initial battery formation process and can prevent further electrolyte decomposition and ensure stable interfacial lithium-ion diffusion. The formation of the SEI involves three main steps: electrolyte solvent/anion reduction, reduction product growth, and SEI layer deposition. 36,37 In situ AFM, as an advanced topographic characterization technique, has been employed to visually observe the formation process of SEI at a nanoscale resolution. For the better resolution of SEI, early in situ AFM studies employed ideal electrodes such as highly oriented pyrolytic graphite (HOPG) and silicon electrodes assembled by chemical vapor deposition, with surface roughness within tens nanometer.38,39

HOPG has been widely used in AFM studies for achieving atomic resolution due to its convenient cleaving procedure, crystalline anisotropy, atomically flat defect-free surface, and highest three-dimensional (3D) ordering.^{20,40} Combining the AFM techniques with cyclic voltammetry (CV) could provide direct evidence and detailed images of SEI formation processes. An early study utilized the in situ electrochemical AFM approach to understanding the SEI live formation (Figure 2A). The HOPG surface with clear edge sites and basal planes exposed was interface-free between the potential range 2.5 and 2.1 V. As the potential decreased to below ~1.5 V, nanoparticles (NPs) gradually accumulated along the edge sites of HOPG, which was attributed to the initial intercalation of solvated lithium ion into the HOPG top graphene layer and ethylene carbonate (EC) reduction. At around 1.0 V, the basal planes of HOPG were engulfed by SEI, which correlated to the significant reduction of carbonate.40

To improve the adaptability of SEI, an ideal electrolyte composed of stable solvent and high ion conductivity lithium salts is urgently needed. 43-46 For instance, the effect of lithium bis(fluorosulfonyl)imide (LiFSI) concentrations to form SEI was studied via the in situ AFM, which revealed that the LiFSI concentration in electrolytes greatly influenced the modulus and thickness of the as-formed SEI layer. The results showed that the SEI layer (~70 nm) formed in 2 M LiFSI/1,2-dimethoxyethane (DME) was thicker than the SEI formed in other electrolyte concentrations. This thickest SEI layer possessed the highest rigid lithium fluoride (LiF) content, which was generated from the FSI⁻ decomposition. Such strong SEI enabled fast lithium diffusion and uniform lithium deposition and protected the lithium anode from electrolyte corrosion.⁴⁷ Due to their incombustibility, excellent ionic conductivity, and high electrochemical and good thermal stability, ionic liquids (ILs) are regarded as promising electrolytes for LIBs. 48,49 In situ AFM was applied to explore the whole SEI generation process (nucleation, growth, and formation) on

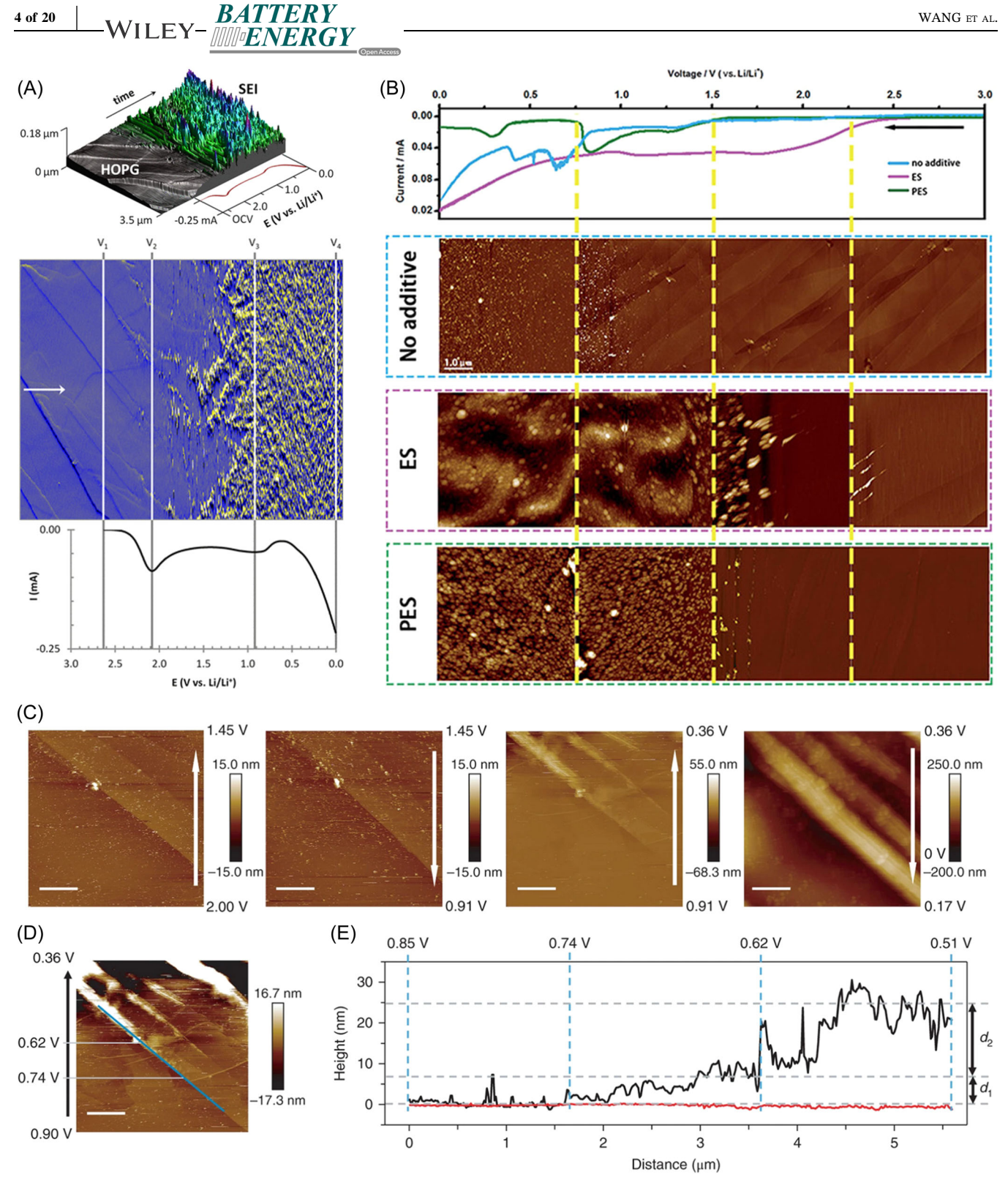


FIGURE 2 (A) Solid-electrolyte interphase (SEI) formation process on a highly oriented pyrolytic graphite (HOPG) surface in 1.5 M LiTFSI/ethylene carbonate (EC) electrolyte during cathodic cyclic voltammetry (CV) scan (scan rate: 5 mV/s). Reproduced with permission. 40 Copyright 2014, American Chemical Society. (B) Cathodic CV curves (scan rate: 2 mV/s) of the HOPG electrode in 1 M LiPF₆/EC/dimethyl carbonate with no additive, 1% ethylene sulfite (ES) additive, and 1% prop-1-ene-1,3-sultone (PES) additive, and corresponding in situ atomic force microscopy (AFM) images demonstrating the evolution of SEI. Reproduced with permission. 41 Copyright 2018, Royal Society of Chemistry. (C) Topological imaging of HOPG during the CV scan (scale bars, 1 μm). (D) Correlation of morphology and potential during the initial cathodic scan (scale bar, 1 µm). (E) Height distribution of SEI along the blue line in (D). Reproduced with permission. 42 Copyright 2019, Nature Publishing Group.

27681696, 2023, 6, Downloaded from https://onlinelibtary.wiley.com/doi/10.1002/bte2.2023006 by Test, Wiley Online Library on [13/09/2024]. See the Terms and Conditions (https://onlinelibrary.wiley.com/terms-and-conditions) on Wiley Online Library for rules of use; OA articles are governed by the applicable Creative Commons License and Conditions (https://onlinelibrary.wiley.com/terms-and-conditions) on Wiley Online Library for rules of use; OA articles are governed by the applicable Creative Commons License and Conditions (https://onlinelibrary.wiley.com/terms-and-conditions) on Wiley Online Library for rules of use; OA articles are governed by the applicable Creative Commons License and Conditions (https://onlinelibrary.wiley.com/terms-and-conditions) on Wiley Online Library for rules of use; OA articles are governed by the applicable Creative Commons License and Conditions (https://onlinelibrary.wiley.com/terms-and-conditions) on Wiley Online Library for rules of use; OA articles are governed by the applicable Creative Commons License and Conditions (https://onlinelibrary.wiley.com/terms-and-conditions) on Wiley Online Library for rules of use; OA articles are governed by the applicable Creative Commons License and Conditions (https://onlinelibrary.wiley.com/terms-and-conditions) on Wiley Online Library for rules of use; OA articles are governed by the applicable Creative Commons License and Conditions (https://onlinelibrary.wiley.com/terms-and-conditions) on the conditions of th

HOPG substrate in IL-based electrolytes. The results indicated that different types of anions in the IL electrolyte significantly influenced the SEI structure. [BMP]⁺[TFSI]⁻-containing LiTFSI, the formed SEI films tended to be loose and rough with a 3D growth mode, while thin and compact SEI films were formed with a twodimensional growth mode in [BMP]⁺[FSI]⁻-containing LiFSI.⁵⁰

The addition of electrolyte additives is regarded as an effective and simplest method for optimizing SEI properties. In situ electrochemical AFM has been employed to monitor the formation process of SEI under different electrolyte systems (with/without electrolyte additives), contributing to analyzing the effect of electrolyte additives on the microstructure of the SEI layer. Since sulfur-containing species are more easily reduced than other components in the electrolyte, they have been reported to facilitate the formation of a stable SEI layer. 51,52 Two sulfur-containing additives, ethylene sulfite (ES) and prop-1-ene-1,3-sultone (PES), were investigated in our previous work.⁴¹ The results suggested that both PES and ES facilitated the SEI formation, in which ES possessed a higher reduction potential. It is worth noting that ES can not only be reduced to form SEI earlier than PES but also formed a denser and more stable SEI to better protect the graphite electrode and improve the stability of the battery (Figure 2B).

Combining in situ AFM with other characterization methods, such as XRD, X-ray photoelectron spectroscopy (XPS), scanning electrochemical microscopy (SECM), neutron reflectometry (NR), Raman spectroscopy, and electrochemical quartz crystal microbalance (EOCM), can provide more comprehensive information on SEI formation process, structure, and composition. For instance, ex situ XPS has been combined with in situ AFM to demonstrate the formation of the hard and dense SEI layer composed of LiF in the LiPF₆/fluoroethylene carbonate/dimethyl carbonate (LiPF₆/FEC/DMC) electrolyte. 46 SECM and in situ AFM were combined in one platform for consecutive investigation of the formation and electrochemical properties of SEI, in which a small area was scratched away via AFM and clearly visualized in the SECM mapping, proving the electronically insulating properties owing to the partially removed SEI.⁵³ The combination of in situ NR and in situ AFM precisely monitored the morphology evolution and the heterogeneities of individual SEI features, in which the scattering length density recorded by NR further provided chemical nature and structural evolution information of SEI.54 Correlative characterization techniques, including in situ AFM, in situ XPS, and in situ Raman, were conducted on both planar and sandwich model lithium batteries during operation to investigate the electrolyte effect on the device performance. The results show that a dense and flat SEI film can be readily generated in a high-concentration electrolyte, demonstrating

good cycling stability and reversibility. The SEI composition derived from the high-concentration electrolyte was further analyzed, which was composed of LiF, Li2S, and Li3N and mainly from the reduction process of FSI^{-.55}

Since EQCM could provide mass change information of electrodes during the discharge/charge process, the combination of EQCM with in situ AFM contributes to a deeper understanding of the complex structure of SEI. Our previous work quantitatively monitored the mass change of interfacial components and recorded real-time topological images of HOPG and SEI height distribution during CV scanning (Figure 2C-E) and confirmed the following distinct stages for SEI formation in 1 M LiPF₆/ EC/DMC electrolyte: formation of LiF (cathodic scan to 1.5 V), Li⁺ co-intercalation (cathodic scan to 0.88 V), the initial reduction of EC (cathodic scan to 0.74 V), further reduction of EC (cathodic scan to 0.6 V), the final reduction of EC (cathodic scan to 0 V and then anodic scan to 0.3 V), and lithium alkylcarbonate reoxidation (anodic scan above 0.3 V).⁴²

Besides the graphite anodes, other different types of anodes, such as alloy-type anodes (Si, Sn, SiO, etc.), lithium metal anodes (LMAs), and metal oxide anodes, are widely studied and considered promising LIB anodes. 56-59

It was reported that in situ AFM was conducted to investigate the effect of FEC additive on the SEI film formation of the commercial SiO/C anode (Figure 3A-C). According to the recorded potential-dependent morphology AFM images and XPS chemical composition analysis results, it was found that a compact, dense, and stiff SEI layer (mainly composed of LiF) was formed on the SiO/C anode surface with the FEC addition. In contrast, only a thin and scattered SEI layer was formed in the EC-based electrolyte. 60 The SEI formation at early stages on the Sn anode in the ECbased electrolyte was studied via the in situ AFM. The results revealed that SEI film was formed at ~2.8 V and then gradually changed in morphology between the potential of 0.7 and 2.5 V. In the following CV cycles, the SEI was not stable and continuously reformed, which could not effectively protect the Sn anode from electrolyte reduction. The interfacial chemistry of the Sn anode and/or the electrolyte needed further optimization.⁶²

Overlithiated organosulfides can form robust SEI and are regarded as promising candidates for LMA protection for stable lithium metal batteries. In situ techniques, including in situ AFM and in situ Raman, were combined to visualize the interfacial evolution (Figure 3D,E) and chemical transformation during the overlithiation process in sulfurized polyacrylonitrile (SPAN). The results showed that the C-S bond broke and the C-Li bond formed during the overlithiation process. The newly formed nucleophilic C-Li further triggered the electrolyte decomposition and hybrid inorganic-organic SEI formation on the SPAN

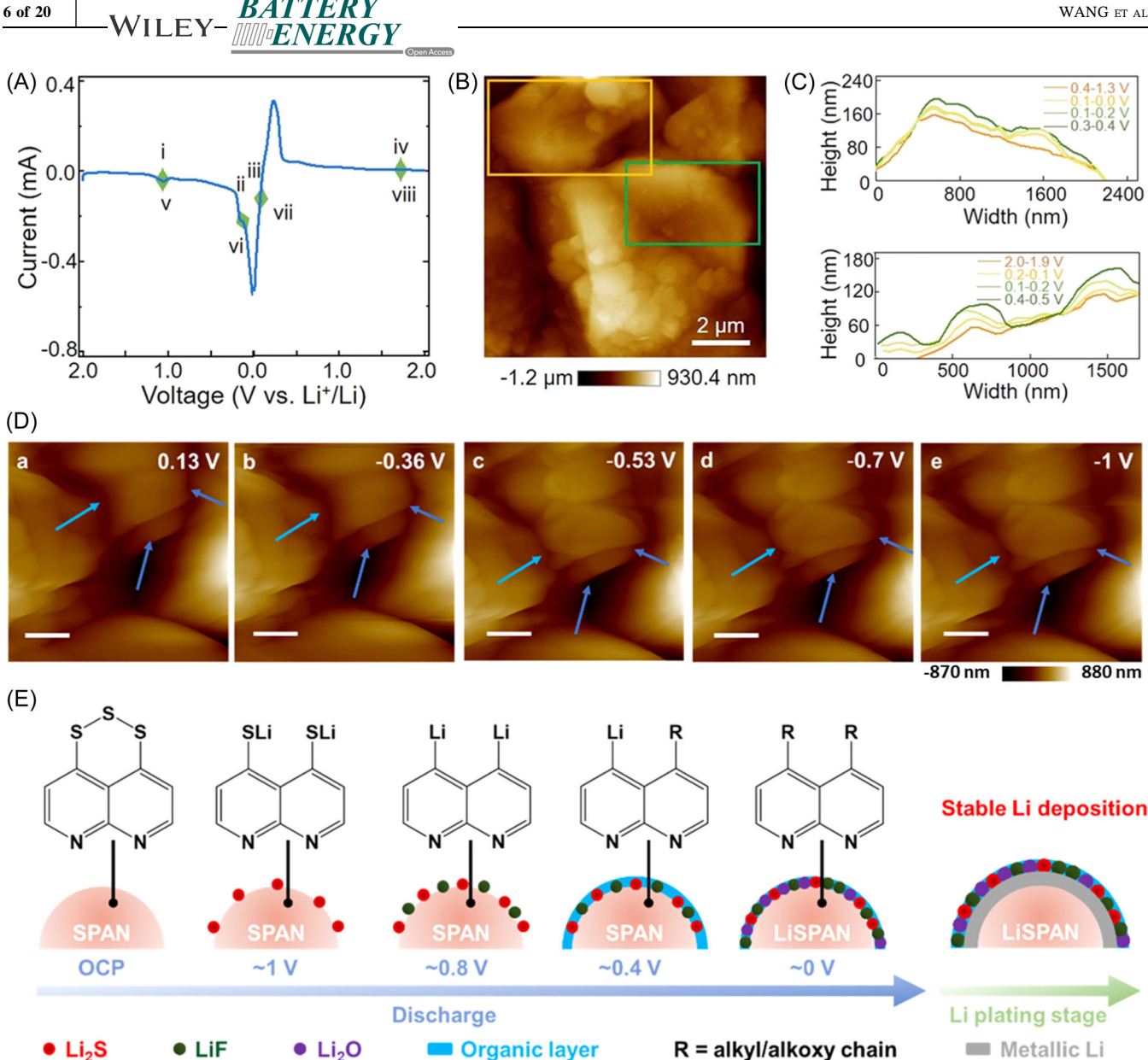


FIGURE 3 (A) Cyclic voltammetry (CV) curve of the SiO/C anode in fluoroethylene carbonate (FEC)-based electrolyte during the in situ atomic force microscopy (AFM) measurement (scan rate: 0.25 mV s⁻¹). (B) AFM image of the anode in the selected area before cycling (orange frame: SiO; green frame: graphite). (C) Line profiles of SiO (top) and graphite (bottom) in selected areas. Reproduced with permission. 60 Copyright 2021, American Chemical Society. (D) In situ AFM monitoring of sulfurized polyacrylonitrile (SPAN) at the lithium deposition stage. (E) Schematic of the mechanism of SPAN during the overlithiation process. Reproduced with permission. 61 Copyright 2021, American Chemical Society.

surface, which contributes to the construction of stable LMAs.61

The direct visualization of SEI layer formation on a Li₄Ti₅O₁₂ (LTO) anode was realized via the in situ AFM technique under potential control. It was found that no SEI was formed on the LTO surface in the EC/DME-based electrolyte between the potential range of 2.5 and 1.0 V. Notably, when the potential was decreased to 0 V, an SEI layer was formed. The effect of different electrolyte additives on the SEI formation was also studied in this work. The results indicated that a dense SEI layer formed with the ES additive and the electrode possessed the smallest polarization with the FEC additive.⁶³ The in situ AFM also provided visual evidence of SEI formation on a Fe₃O₄ anode during the discharge/charge process. The recorded AFM images demonstrated that the as-formed SEI layer in the FEC-based electrolyte was more compact and stable than that as-formed in the EC-based electrolyte. This dense film could efficiently prevent the Fe ion migration and further improve the battery performance.⁶⁴

2.2 | CEI

CEI is generally considered to be a heterogeneous multicomponent film formed due to the decomposition of electrolytes on the cathode surface. However, compared with the extensive study of SEI, the investigation of CEI is comparatively insufficient. The complexity of CEI structure brings great challenges to developing stable CEI layers, so the study of the formation mechanism and properties of CEI plays a key role in improving the capacity, cycle life, and overall safety of batteries.⁶⁵

In situ AFM has been applied to observe the evolution of CEI on LiCoO₂ cathode during electrochemical cycling. The results suggested that CEI films only formed on the edge plane of the LiCoO₂ cathode with loose fibrillar structures, which were unstable and decomposed at low voltage (Figure 4A). This loose structure could not completely coat the edge plane or block further oxidation of the electrolyte or protect the LiCoO₂ from a trace amount of HF in the electrolyte, which was detrimental to the battery cycling and performance. To enhance the stability in high-voltage cycling, a thin layer of Al₂O₃ was coated on the cathode surface, which successfully suppressed the formation of CEI at the LiCoO₂ edge plane and demonstrated significantly improved cycle stability at high voltage.⁶⁶

The surface regulation and dynamic degradation of single-crystalline Ni-rich cathode (SC-NCM) within solidstate lithium batteries (SSLBs) was investigated via the in situ AFM. Unstable and inhomogeneous CEI film with surface defects was observed on SC-NCM electrodes during the cycling process. To solve this issue, the Li₃PO₄ coating layer was introduced to the SC-NCM electrodes to mediate their surface structure and CEI evolution process. First, the cell with Li₃PO₄-coated SC-NCM electrodes (L-NCM) was held at ~4.08 V for 1 h, and some amorphous products were gradually formed on the L-NCM surface. As the charging process proceeded, these amorphous products accumulated and evolved into the planar amorphous film. When the potential increased to 4.2 V, the homogenized film ultimately formed on the L-NCM surface. After cycling, this film became denser and smoother and covered the entire L-NCM surface (Figure 4B-D). Notably, this amorphous LiF-rich CEI well maintained its structure during the subsequent cycling process, which suppressed undesired side reactions and enhanced the interfacial stability, further contributing to the cycle life stability and rate capability enhancing.²⁷

A facile protocol was developed to in situ observe and characterize a single-particle electrode via in situ AFM. It was discovered that the formation of CEI on the $LiNi_{0.5}Mn_{1.5}O_4$ particle cathode surface was highly related to the exposed planes. The CEI film with a thickness of 4–5 nm was formed on the (111) surface at ~4.78 V and

maintained stable when the potential decreased. In contrast, no detectable CEI film was generated on the (100) surface during the first cycle. This work suggested that the interfacial catalytic activity of electrolyte oxidation is closely related to the facet properties.⁶⁷

The in situ AFM was applied to investigate the CEI changes in high-energy-density lithium- and manganese-rich (LMR) materials. It was found that a dense and uniform passivation CEI film was formed on the LMR material surface at high voltage. Further, XPS characterization confirmed that the CEI was composed of LiF. The as-formed stable LiF-rich CEI film inhibited the electrolyte oxidation, thus suppressing the generation and accumulation of $\rm CO_2$ on the LMR material surface. The battery (LMR||Li) test demonstrated that the formed CEI film significantly improved the battery rate and cycling performance in the commercial carbonate electrolyte. 68

3 | MECHANICAL PROPERTIES

The mechanical degradation process of electrode materials plays an important role in limiting the lifetime of advanced LIBs. For instance, the repetitive intercalation and deintercalation of ions during discharge/charge induced the volume expansion and contraction of electrodes under fatigue loading conditions, which leads to electrode fracture/ breakage and further affects the battery energy storage capacity and cycle life. 69,70 Therefore, measuring and understanding the mechanical properties and evolution of electrode materials during the discharge/charge process, such as fracture strength and Young's modulus (YM), is of great significance for achieving long-cycle-life batteries. Due to the convenience of measuring force and displacement using an AFM tip, AFM has been widely applied to study and measure the mechanical properties of electrode materials, such as YM, fracture strength, stiffness, and adhesion.^{71–74} Combining with electrochemical testing, the mechanical behaviors of electrode materials upon the battery cycling process can be investigated via the in situ AFM techniques.

The mechanical changes of the SEI layer at the HOPG and graphite anodes were investigated by in situ AFM. HOPG was first studied as a model system to explore the SEI formation and corresponding mechanical property evolution. Then industry-relevant graphite sheet was further investigated (Figure 5A). It was found that two types of SEI simultaneously formed at the basal and edge planes of graphite; meanwhile, the thickness of SEI in the edge site was bigger than that in the basal plane. The addition of FEC and vinylene carbonate in 1 M LiPF₆/EC/ethylmethyl carbonate (EC/EMC) electrolyte increased YM and reduced

27681696, 2023, 6, Downloaded from https://onlinelibrary.wiley.com/doi/10.1002/bte2.2023006 by Test, Wiley Online Library on [13.09/2024]. See the Terms and Conditions (https://onlinelibrary.wiley.com/terms

and-conditions) on Wiley Online Library for rules of use; OA articles are governed by the applicable Creative Commons License.

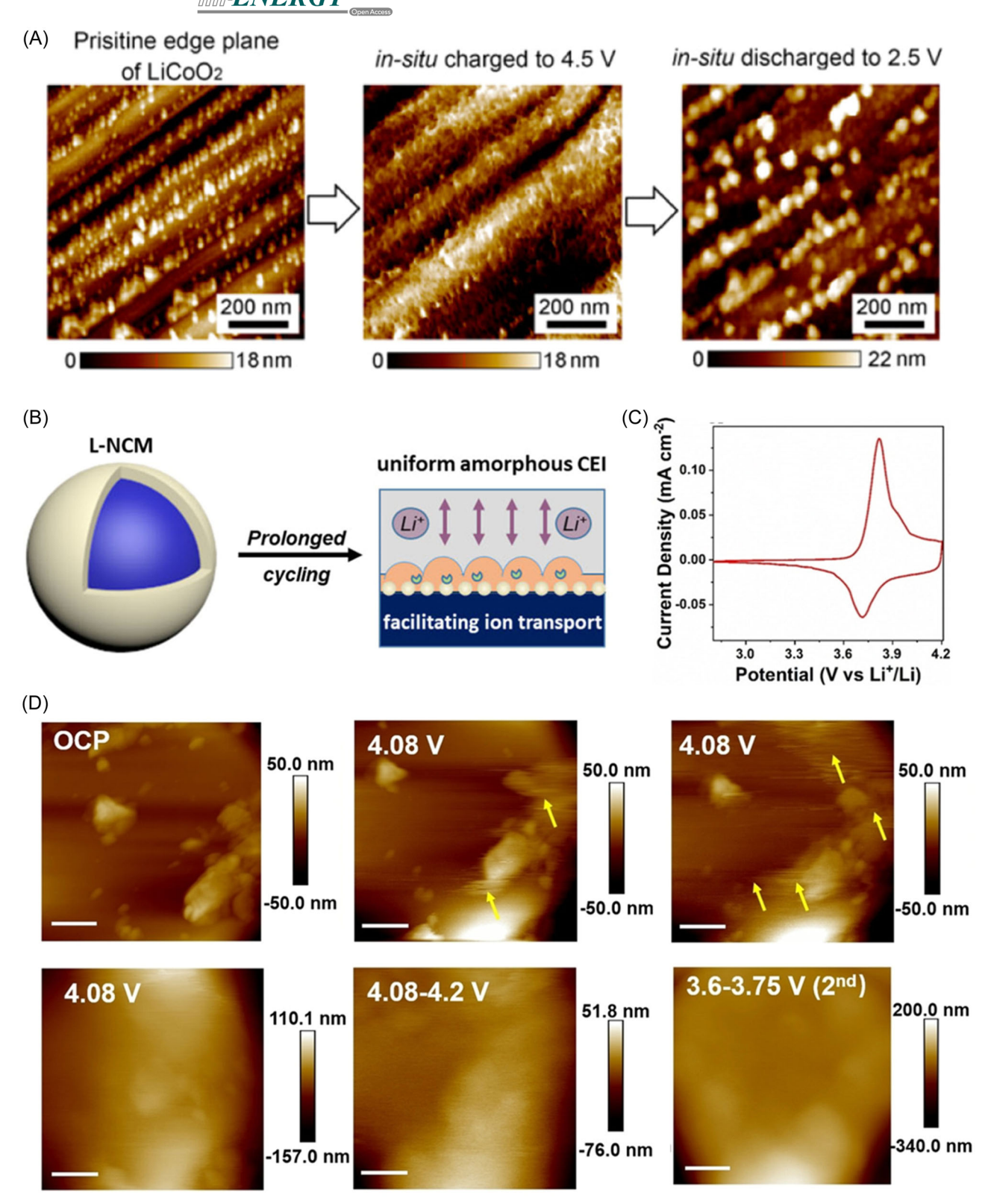


FIGURE 4 (A) In situ atomic force microscopy (AFM) images of the cathode–electrolyte interphase (CEI) film formation and decomposition on the edge plane of $LiCoO_2$ crystal. Reproduced with permission. Copyright 2017, American Chemical Society. (B) Schematic illustration of the surface degradation and interfacial regulation mechanism of the Li_3PO_4 -coated single-crystalline $LiNi_{0.5}Co_{0.2}Mn_{0.3}O_2$ (NCM523) (L-NCM) electrodes. (C) The first cycle of cyclic voltammetry (CV) curves (scan rate: 0.1 mV/s) and (D) corresponding in situ AFM images demonstrate the surface evolution of CEI film on the L-NCM cathode electrode in a solid-state lithium battery. Reproduced with permission. Copyright 2022, John Wiley and Sons.

27681696, 2023, 6, Downloaded from https://onlinelibrary.wiley.com/doi/10.1002/bte2.2023006 by Test, Wiley Online Library on [13/09/2024]. See the Terms and Conditions (https://onlinelibrary.wiley.com/terms-and-conditions) on Wiley Online Library for rules of use: OA articles are governed by the applicable Ceravive Commons License

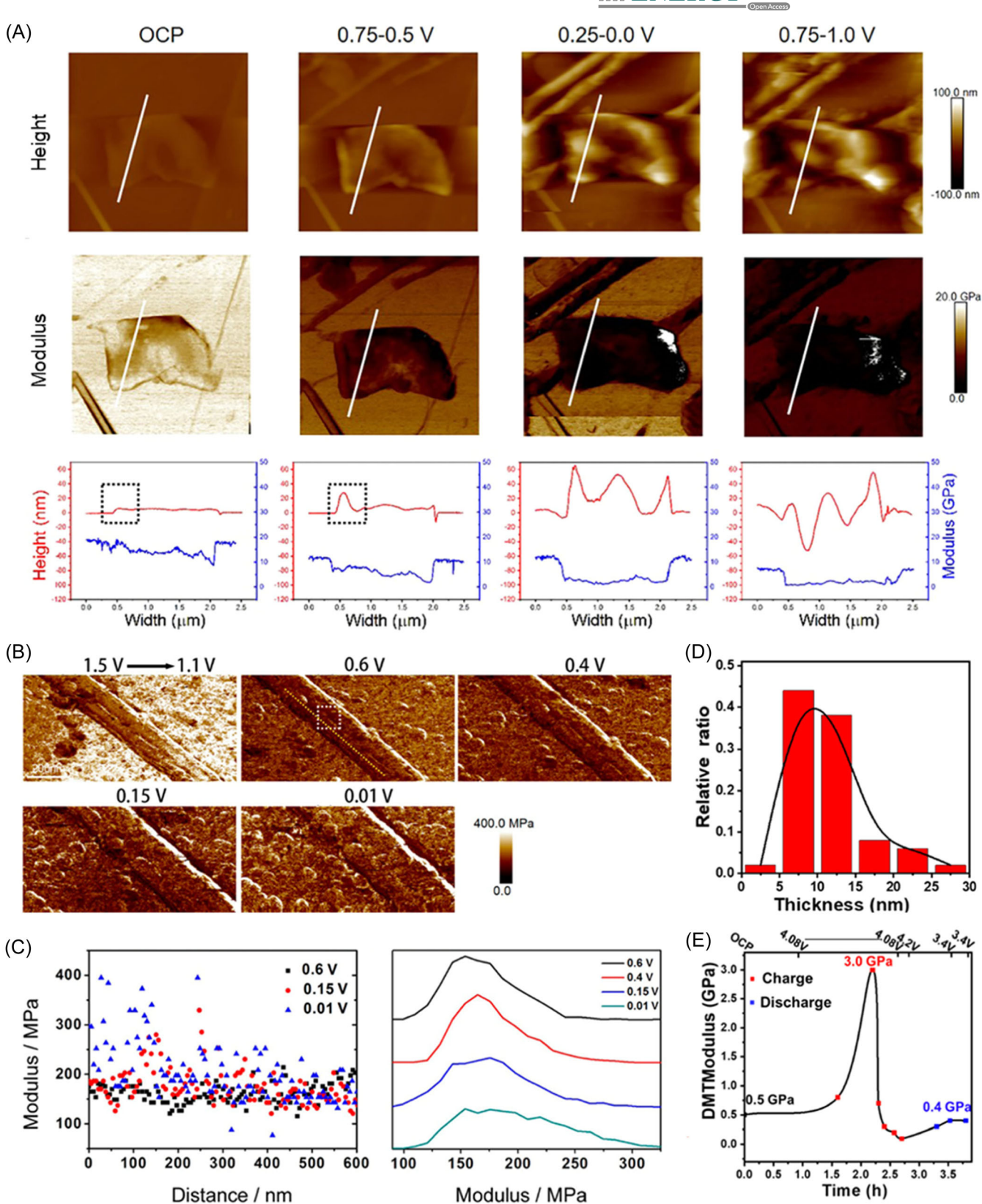


FIGURE 5 (See caption on next page).

SEI thickness and roughness, thus further enhancing the battery performance. Due to its high edge-to-basal ratio, the individual graphite anode showed a lower SEI modulus and more SEI covering, compared to the HOPG. The different material structures (strain behavior, the density of step edges, etc.) of HOPG and graphite further lead to different device performances.²⁶

Due to its natural abundance, high specific capacity, and relatively low working potential, silicon has been considered a promising anode material for LIBs. 77,78 Huge volume change during cycling and derived mechanical stress bring great troubles to maintaining electrode and SEI structure integrity, which leads to undesirable fast performance degradation. 79,80 The studies that focused on the interfacial behavior and electrochemical reactions of silicon anode are of great importance for improving battery performance and stability. In situ AFM was used to investigate the SEI growth and mechanical properties of a silicon nanowire electrode, which quantitatively tracked YM and morphology changes during the SEI growth process.⁷⁵ Three distinct stages were observed during the SEI growth process. Figure 5B shows the recorded in situ YM mapping of the Si nanowire. At the initial discharge stage, the YM of the Si nanowire surface was around 700 MPa. When the voltage was reduced to 0.6 V, the YM decreased to ~150 MPa, which was attributed to the newly formed primary SEI film during discharge. The YM and morphology remained unchanged when discharged to 0.4 V. In the second stage (discharged to 0.15 V), a thick and particle-like SEI formed with slightly increased and inhomogeneous YM. In the final stage (further discharged to 0.01 V), the YM became more inhomogeneous. Furthermore, the YM of the selected position was analyzed to study its distribution and trend during the SEI growth process (Figure 5C). During the growth process, the YM increased obviously and became more inhomogeneous. Meanwhile, the statistical mean value and distribution of YM during the growth process showed a slight increase, suggesting the composition evolution of SEI films. The mechanical evolution on the cross-section of microsized silicon anode was successfully visualized via the in situ AFM, including initial pulverization, irreversible volumetric changes, the onset of particle crack formation and its patterns, fresh SEI formation

at cracked surfaces, and particle isolations. The results indicated that the upper cutoff voltage could suppress the mechanical failure of the microsized silicon anode and subsequently improve capacity retention with a reduced cell impedance. 81

In situ AFM has also been utilized to disclose the mechanical properties and interface evolution of CEI. For instance, the dynamic formation of CEI on LiNi_{0.5}Co_{0.2}Mn_{0.3}O₂ (NCM523) electrode in an SSLB was monitored via the in situ AFM.⁷⁶ The average Derjaguin-Muller-Toporov (DMT) modulus of the NCM523 electrode surface was 0.5 GPa at the open-circuit potential (2.85 V). No evident morphology and DMT modulus changes were observed when charged to 4.08 V. Then, the SSLB was held at 4.08 V for 1.2 h, in which some filamentous products first appeared accompanied by the DMT modulus increase to 3 GPa, and then some flocculent products deposited accompanied by DMT modulus decrease to 0.5 GPa. As the charging process proceeded, the products evolved into a flocculent film with a low DMT modulus (0.3 GPa). At the following charging process (to 4.2 V), no significant changes were observed in terms of DMT modulus and morphology. Then, the SSLB discharged to 3.4 V, and the film became denser and smoother with a slight increase in DMT modulus (to 0.4 GPa). Furthermore, the film thickness was measured from the analysis of the recorded AFM images (Figure 5D). The results showed that the film thickness was around 11.18 nm. The DMT modulus evolution of the selected position is demonstrated in Figure 5E. Notably, the DMT modulus was stable during the SSLB cycling process. suggesting the mechanical property of this film turned stable after the first cycle. The real-time visualization of the CEI growth via in situ AFM provides more details and evidence of the interfacial behavior and mechanical properties, further contributing to the development of SSLB.

4 | MORPHOLOGICAL CHANGES

The studies of electrode morphological changes in LIBs, including dimensional changes (height and volume), morphological evolution, and topography changes, play a vital

FIGURE 5 (A) In situ atomic force microscopy (AFM) of an individual graphite sheet on the highly oriented pyrolytic graphite (HOPG) substrate in the electrolyte of ethylene carbonate/ethylmethyl carbonate (EC/EMC). Height and modulus information of four potential steps (open-circuit potential [OCP], 0.75–0.5, 0.25–0.0, and 0.75–1.0 V). Reproduced with permission. Copyright 2020, American Chemical Society. (B) The AFM images of Young's modulus mapping of a single silicon nanowire (SiNW) anode in the first discharge process. (C) The distribution of Young's modulus along the location marked with a dashed yellow line (left), and the statistic values of Young's modulus of the area marked with a dashed white box (right). Reproduced with permission. Copyright 2014, American Chemical Society. In situ AFM of the LiNi_{0.5}Co_{0.2}Mn_{0.3}O₂ (NCM523) electrode surface during charge and discharge. (D) The Gauss statistic distribution histograms of the film thickness and (E) quantitatively measured average Derjaguin–Muller–Toporov (DMT) modulus of the selected position during charge/ discharge. Reproduced with permission. Copyright 2020, American Chemical Society. OCP, open-circuit potential.

role in a deep understanding of the battery mechanism. In this section, we mainly discussed the morphological changes for different types of anodes and cathodes of LIBs, which were obtained through in situ AFM.

Due to their high theoretical capacity, alloy anode materials that can be alloyed with lithium ions, such as Si and Sn, are considered promising LIBs anode. However, the volume changes (expansion/contraction) of alloy anodes during the lithiation/delithiation process led to electrode structural degradation, further degrading the battery performance. Therefore, investigating the morphological changes of alloy anodes is of great importance for developing effective methods to stabilize the alloy anodes.82-86

For instance, in situ AFM was applied to quantitatively and qualitatively monitor the morphological evolution of different nanosized amorphous Si (a-Si) nanopillars (height: 100 nm; diameters: 100-1000 nm) during the lithiation and delithiation processes (Figure 6A,B). The nanopillars with a diameter of 100 nm had a volume expansion smaller than 200%. The nanopillars with a diameter bigger than 100 nm all reached a large volume expansion of around 300%. All the nanopillars were roughened with no crack after five cycles. As the cycling process proceeded, the nanopillars with a

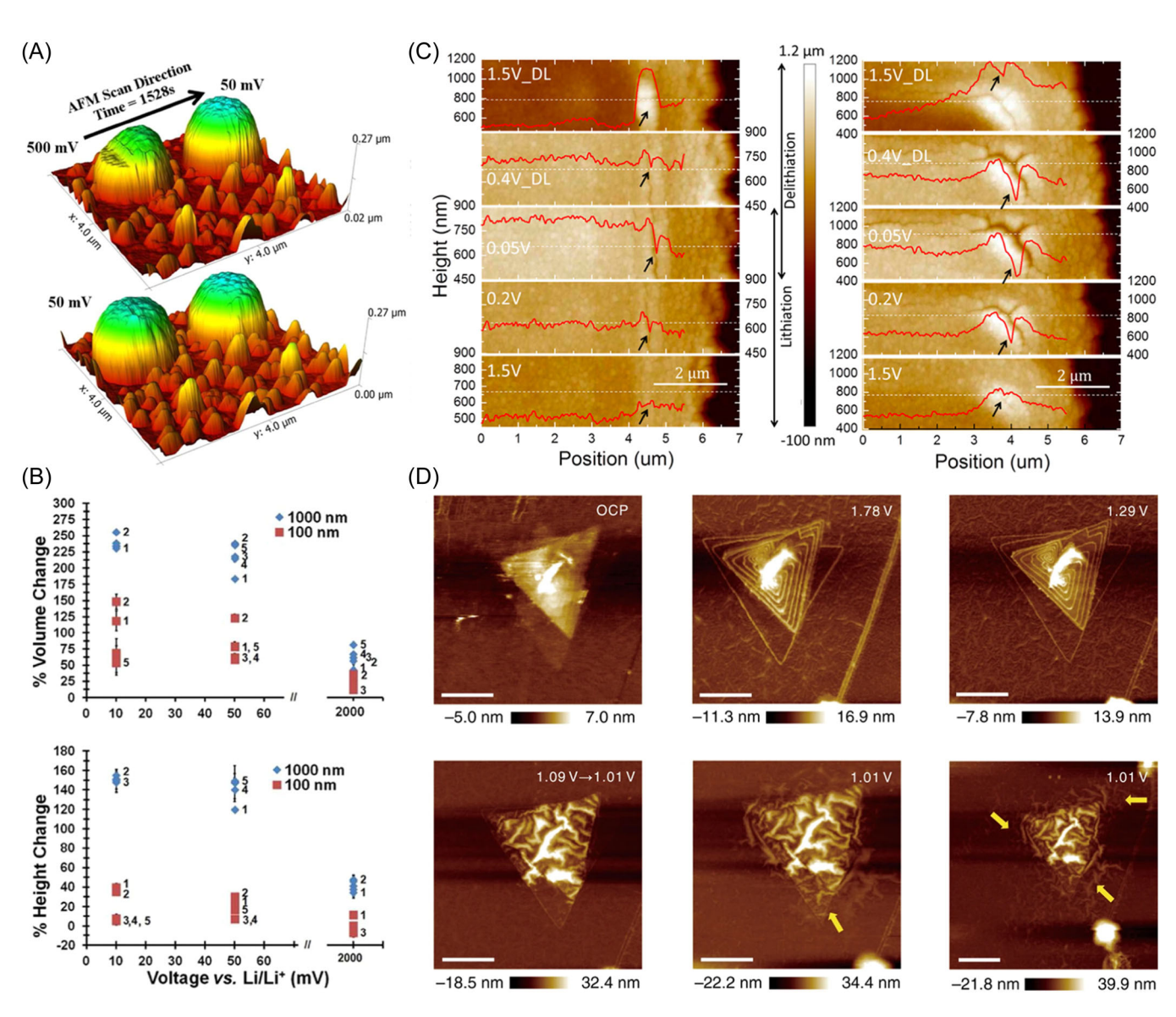


FIGURE 6 In situ atomic force microscopy (AFM) of lithiation and delithiation of amorphous Si (a-Si) nanopillars: (A) AFM images of the growth of the a-Si nanopillars (100 and 1000 nm) during the electrochemical cycling (scan rate: 1 mV/s). (B) Height and volume changes of five cycles. Reproduced with permission. 87 Copyright 2013, American Chemical Society. (C) Crack evolution of a patterned a-Si electrode at the edge (left) and corner (right) during the third cycle. Reproduced with permission. 88 Copyright 2016, American Chemical Society. (D) In situ AFM images of the interfacial morphologies evolution on a multilayer triangular molybdenum disulfide (MoS₂) electrode. Reproduced with permission.⁸⁹ Copyright 2019, Nature Publishing Group.

27681969, 2023, 6, Downloaded from https://onlinelibrary.wiley.com/doi/10.1002/bte2.2023006 by Test, Wiley Online Library on [13/9/92024]. See the Terms and Conditions (https://onlinelibrary.wiley.com/terms-and-conditions) on Wiley Online Library for rules of use; OA articles are governed by the applicable Creative Commons Licenses

diameter of 100 and 200 nm were kept intact, while the nanopillars with a diameter of 300 nm cracked after 27 cycles. This real-time qualitative examination of the morphological (height and volume) changes of the a-Si nanopillars motivates future studies to quantify the structural integrity changes of Si nanopillars.⁸⁷ In situ AFM has also been utilized to observe the influence of volume expansion/contraction of Si electrodes in the mechanical degradation of SEI (Figure 6C). It was found that the SEI was tensed when the Si electrode expanded, which induced crack formation in the surface layer. Then, the cracks were not fully filled in at the low potential and further reopened and closed in the next cycles. This work directly monitored the SEI fracture process, which contributes to the chemical–mechanical degradation studies and capacity fade predictions of LIBs.⁸⁸

In addition to the Si materials, molybdenum disulfide (MoS₂) is also considered a promising LIBs anode material due to its high theoretical specific capacity. However, the SEI of the MoS₂ anode is unstable; therefore, the study of the structural evolution of the MoS₂ anode is crucial for battery performance improvement. It was reported that in situ AFM has been employed to monitor the dynamic lithiation/delithiation and SEI film formation on the large-area ultra-flat monolayer MoS₂ electrode. As shown in Figure 6D, the triangular MoS₂ had a layer spacing of ~0.7 nm at open circuit potential. When the potential decreased to 1.29 V, the electrode/electrolyte interface remained unchanged. Notably, when the potential decreased from 1.09 to 1.01 V, the triangular MoS₂ suddenly wrinkled, indicating the flexibility of the MoS2 anode. As the lithiation proceeded, the bottom side of the triangular MoS₂ also wrinkled and then spread from the defect sites to the surrounding places. However, during the following discharging process, the as-formed wrinkles did not completely return to the original flat shape and the volume expansion was irreversible either. This work revealed the influence of surface defects on reaction kinetics, which contributes to a deeper understanding of structure-reactivity relationships.89

The morphological evolution and dynamic mechanism (dynamic pathway and degradation mechanism) of the lithium and lithium-indium alloy anodes in the $\text{Li}_{10}\text{GeP}_2\text{S}_{12}$ -based all-solid-state Li metal batteries were investigated via the in situ AFM techniques (Figure 7A). Due to the low ionic migration barrier and fast ionic diffusion coefficient of the lithium-indium alloy anode, a homogeneous SEI shell was formed on this alloy anode, which further induced the uniform growth of Li_xIn lamellae during the lithiation process. Furthermore, the volume and surface area of the wrinkling structure were quantitatively analyzed, which suggested the breathing phenomena of the cycling behavior during the

lithium-indium dealloying/alloying processes, enabling favorable inner lithium accommodation.⁹⁰

Besides the real-time monitoring of lithium-ion intercalation behavior in LIBs, the real-time observation of intercalation/deintercalation processes in dual ion batteries (DIBs) was also achieved via the in situ AFM (Figure 7B,C). Through measuring the distance changes between graphene layers during the intercalation process, it was found that PF6 $^-$ intercalated in one of every three graphite layers with a speed of $\sim\!\!2\,\mu\mathrm{m}\!\cdot\!\mathrm{min}^{-1}$. At high voltages, the graphite wrinkled and suffered structural damage with electrolyte decomposed on its surface, leading to the cycling performance degradation of DIBs. 33

5 | SURFACE EVOLUTION

In situ AFM has also been applied to directly visualize the surface evolution of electrodes with high spatial resolution, such as the dendrite formation during lithium anode plating and stripping processes, ^{91–94} and the deposition and dissolution/decomposition of intermediates/reaction products on the cathode surface of the lithium–sulfur batteries ^{30,95–98} and lithium–oxygen batteries. ^{31,99–102}

The ununiform lithium stripping and plating upon cycling induced the dendrite formation on the lithium anodes, which reduced the battery performance and even potentially caused the short circuit, further leading to safety problems. Therefore, studying the dendrite formation process on the lithium anode surface is crucial for improving battery design and safety. In situ AFM measurements have been conducted to directly visualize the lithium stripping and plating process on the pristine lithium anode and lithium polyacrylic acid (LiPAA) SEI layer-modified lithium anode (Figure 8A). The SEI on the pristine lithium anode surface was not stable and was destroyed by the dynamic lithium stripping/plating behavior, further causing the side reactions and dendrite formation. Notably, after applying a smart LiPAA SEI with good stability and high bonding ability, the uneven stripping/plating behavior was markedly reduced, and the side reactions were greatly reduced with significantly improved battery safety.⁹² In situ AFM has also been reported to provide insights into the lithium nitrateregulated lithium stripping/plating process in gel polymer electrolyte (GPE)-based lithium metal batteries at the nanoscale. Amorphous nitride SEI was formed due to the addition of lithium nitrate, which facilitated lithiumion diffusion, stabilized a compatible interface, and regulated the lithium nucleation/growth. The deposited lithium was compact. The lithium dissolution exhibited good reversibility, ensuring the cycling performance of

27681696, 2023, 6, Downloaded from https://onlinelibrary.wiley.com/doi/10.1002/bte2.2023006 by Test, Wiley Online Library on [13/09/2024]. See the Terms and Conditions (https://onlinelibrary.wiley.com/derms/

and-conditions) on Wiley Online Library for rules of use; OA articles are governed by the applicable Creative Commons License.

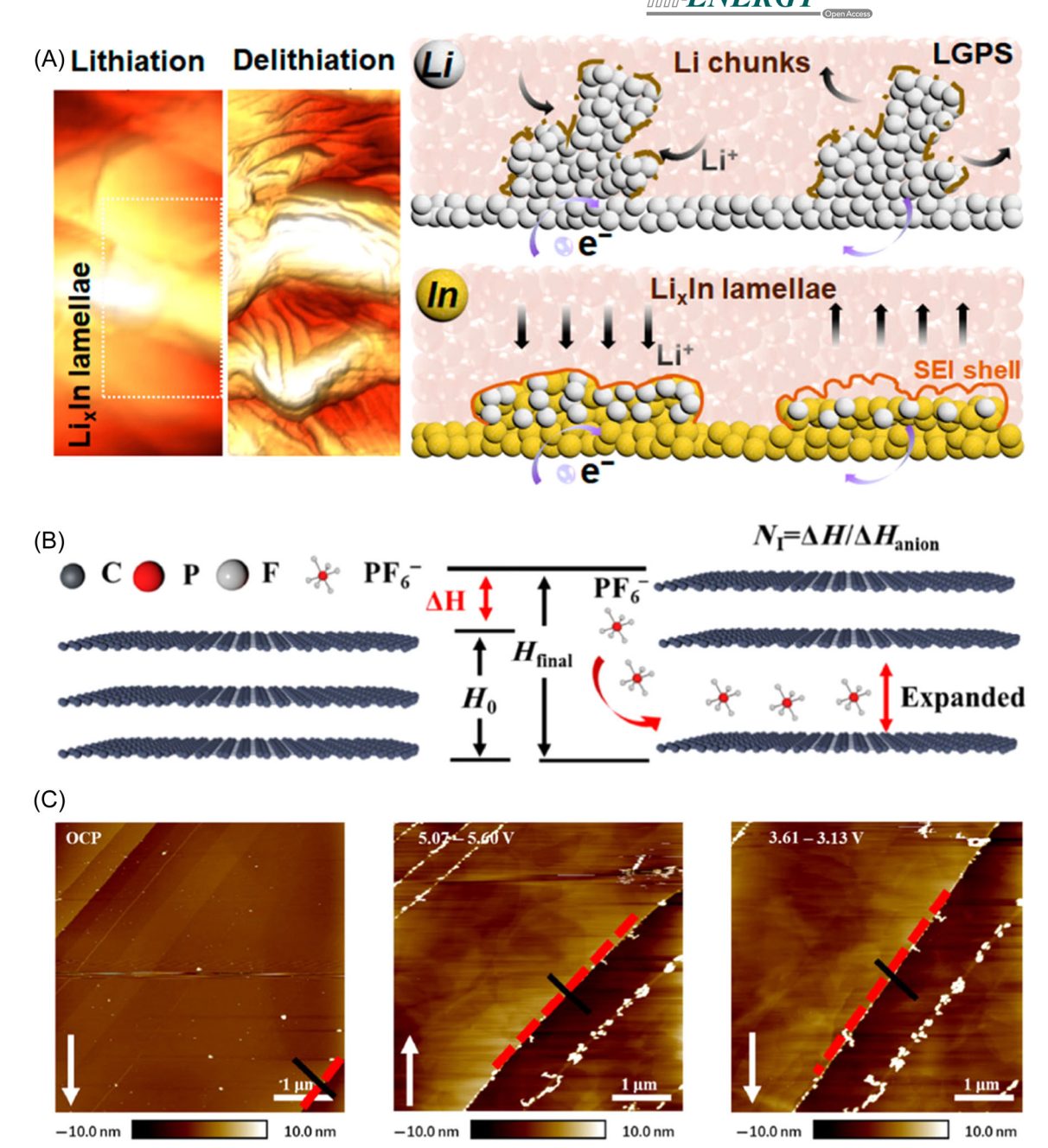


FIGURE 7 (A) Atomic force microscopy (AFM) images of LixIn lamellae at lithiation and delithiation states and schematic of the interfacial mechanism of lithium electrode (top) and indium electrode (bottom). Reproduced with permission. Opyright 2021, American Chemical Society. (B) Description of parameters related to the PF₆⁻ anion intercalation process of highly oriented pyrolytic graphite (HOPG) in carbonate electrolyte. (C) In situ AFM images of HOPG anode in carbonate electrolyte at different voltages. Reproduced with permission. 3 Copyright 2020, Tsinghua University Press and Springer-Verlag GmbH Germany, part of Springer Nature. LGPS, Li₁₀GeP₂S₁₂.

lithium metal batteries. 93 In situ AFM was also applied in the monitoring of initial lithium deposition in FEC-based and EC-based electrolytes on graphite anodes for understanding the lithium dendrites growth evolution processes at the nanoscale. The results showed that a denser and harder LiF-rich SEI layer was formed in the FEC-based electrolyte, which sufficiently impeded the lithium ion reduction and deposition on the anode

surface and suppressed dendrite growth. 103 The dynamic Li plating/stripping behaviors upon cycling at the gel polymer electrolytes/lithium metal electrode interface in the quasi-solid-state lithium metal batteries were monitored by in situ AFM. Uneven lithium deposition with cavity-shaped defects and partial dissolution was observed at the lithium metal and gel polymer electrolyte interface. Furthermore, the addition of LiNO3 induced

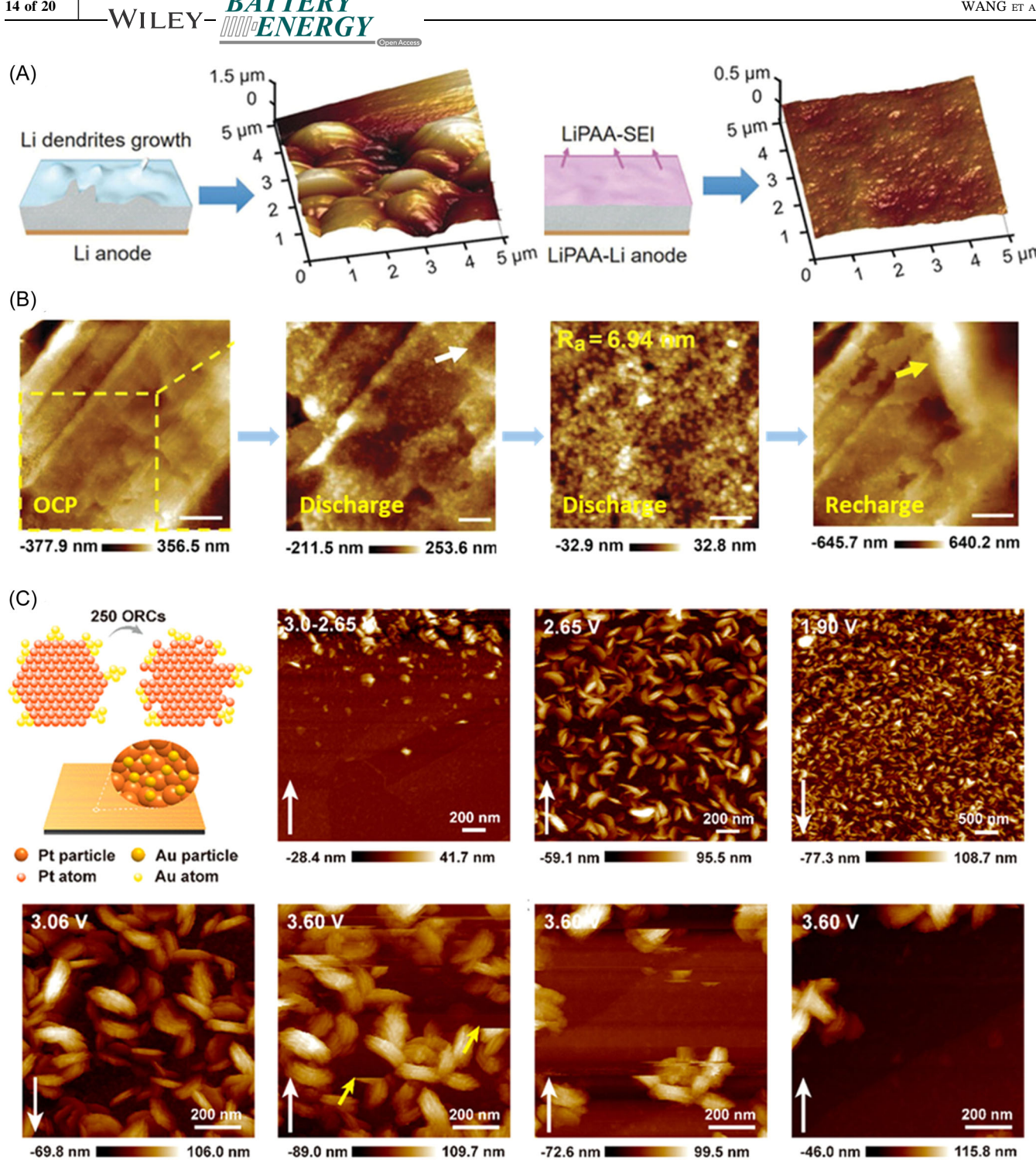


FIGURE 8 (A) Schematic and atomic force microscopy (AFM) images of pristine Li anode (left) and lithium polyacrylic acid-Li (LiPAA-Li) anode (right) after the lithium stripping process. Reproduced with permission. ⁹² Copyright 2017, John Wiley and Sons. (B) In situ AFM monitoring of the Li anode surface evolution in a quasi-solid-state lithium-sulfur (QSSLS) cell containing 5 wt% LiNO3. Reproduced with permission. 6 Copyright 2022, John Wiley and Sons. (C) In situ AFM images on the Pt/Au nanoparticle electrode surface upon the discharge/charge process in a Li-O₂ model cell. Reproduced with permission. ¹⁰⁰ Copyright 2021, American Chemical Society. OCP, open-circuit potential; SEI, solid-electrolyte interphase.

the formation of SEI film and homogeneous lithium deposition/dissolution. It also demonstrated good reversibility of lithium metal upon the lithium plating/ stripping process.93

The back and forward diffusion of polysulfide between the anode and cathode of lithium-sulfur batteries is called the shuttle effect, which can lead to severe corrosion of the lithium anode and irreversible capacity loss of batteries. Thus, direct characterization of the deposition and dissolution processes of the lithium sulfide intermediates is of great significance in understanding polysulfide shuttle mechanisms and facilitating its improvement. For instance, in situ AFM was utilized to monitor dynamic processes and interfacial properties on the additive-mediated lithium anode surface at the nanoscale. After adding lithium nitrate to the electrolyte, two SEI formation stages were detected. First, loose NPs (~102 nm) were formed at the OCP. Then, dense NPs (~74 nm) were formed during the discharge process, caused by the synergistic effect of lithium nitrate and lithium polysulfides (Figure 8B). The as-formed dense SEI film can not only prevent the erosion of lithium polysulfides but also homogenize the lithium deposition behavior, thereby improving the electrochemical performance of lithium-sulfur batteries. 96 The investigation of the interfacial behavior at a high temperature (60°C) in lithium-sulfur batteries, including the dynamic evolution of insoluble Li₂S and Li₂S₂, was realized via the in situ AFM. An in situ-formed functional film was detected after Li₂S nucleation upon discharge at 60°C. This as-formed film reduced the lithium-ion transport distance between the higher order sulfides and lower order sulfides, promoted the oxidation of Li₂S₂ and Li₂S upon the charge, and facilitated the interfacial morphology maintenance after cycling, which provides insights into the benign interface conservation and the performance optimization of lithium-sulfur batteries.³⁰

For lithium-oxygen batteries, the sluggish decomposition of discharge products (Li₂O₂) led to large overpotential and poor cycling stability. The side reactions and instability of the aprotic electrolyte further degraded the battery performance. Monitoring the generation and decomposition of reaction products during the oxygen reduction reaction (ORR) and oxygen evolution reaction (OER) is crucial for understanding the correlations between the products' morphology and catalytic activity. In situ AFM has been applied to record the dynamic surface evolution of the Pt NP electrode in lithium-oxygen batteries (Figure 8C). The pristine platinum NPs promoted the nucleation and growth of Li₂O₂ nanosheets with reduced overpotential. As the cycling proceeded, the platinum particle size gradually increased and induced cracks on the electrode surface. Meanwhile, the morphology of Li₂O₂ evolved into a larger toroidal structure with degraded reversibility and capacity. After modifying the Pt electrode with a certain amount of gold NPs, the stability of the electrode increased. No obvious particle accumulation and cracks were observed on this gold-modified Pt electrode after 250 cycles, indicating that gold inhibited the morphological evolution of platinum and improved the stability of

platinum without catalytic activity degradation. ¹⁰⁰ In situ AFM has also been employed to record the real-time images of surface evolution on a gold electrode in the lithium-oxygen batteries, which revealed the correlations between ORR and OER catalytic activity and the nanostructure of the gold electrode. The results indicated that nanoporous gold facilitated the nucleation and growth of Li₂O₂ discharge products, while the densely packed gold NPs promoted the full decomposition of Li₂O₂. These observations shed light on the mechanism of nanostructure catalyst-based lithium-oxygen batteries and provide strategies for improving lithium-oxygen batteries. 101

SUMMARY AND OUTLOOK

Developing advanced high spatial and temporal resolution in situ characterization techniques is crucial for understanding the operation, degradation, and failure mechanism of lithium-based batteries. In this paper, we reviewed the application of in situ AFM in LIBs, lithium-sulfur batteries, and lithium-oxygen batteries, including the studies of electrode-electrolyte interfaces, mechanical properties, morphological changes, and surface evolution, which contributes to the electrode and electrolyte optimization and battery performance improvement. Future perspectives of the in situ atomic force techniques in battery characterization are demonstrated as follows:

- (1) Developing in situ electrical properties characterization: In addition to the as-mentioned progress of in situ AFM, other SPM techniques are also considered promising methods to explore the interfacial process and operation mechanism of lithium-based batteries. For example, electrochemical strain microscopy can measure the localized, electrochemically induced volumetric strain, which provides real space mapping of lithium-ion diffusion and contributes to understanding the role of grain defects/orientation in lithium-ion transport. 104-106 Scanning ion conductance microscopy can simultaneously and fast scan the topography and map the variation in electrochemical activity. 107,108 Kelvin probe force microscopy could obtain a high-resolution mapping of electrochemical surface potentials. 109-111 Due to the advantages and limitations of each SPM technique, it is significant that various SPM methods can be combined to investigate the materials, interfaces, and processes of lithium-based batteries.
- (2) Integration of multidimensional characterization: Considering the complicated physical-chemical

reactions in battery systems, the other future direction is combining other advanced characterization methods to acquire the real-time composition changes during the electrochemical process of lithium batteries, such as XRD, XPS, and Raman, which is beneficial for systematically understanding the underlying mechanism of batteries and guiding its design and performance improvement. These developed novel in situ SPM techniques could also be applied beyond the lithium system, such as sodium-ion batteries, potassium-ion batteries, and magnesium-ion batteries, providing a useful tool to realize the development of high-performance battery systems and meet the increasing energy demand.

- (3) Operando characterization under various operation conditions: AFM observation on real electrodes should be further carried out to reveal the practical reaction mechanism. Besides, multifunctional in situ cells should be designed to enable the testing under different operation conditions of LIBs (such as under high/low temperatures, under different working gas and liquid, electrolyte and gas circulation systems, and electrical and mechanical abuse conditions).
- (4) Advanced electrode manufacturing techniques: Microand nanofabrication technologies (such as photoetching, electron beam evaporation, and 3D printing) should be further introduced to develop various electrode structures that simulate the reaction process in different battery systems. Besides, interface pretreatment techniques (such as ion beam etching and plasma etching) should also be widely employed to create an optimized interface for AFM characterizations.
- (5) Artificial intelligence-assisted AFM analysis: Advanced computational and algorithmic techniques should be introduced for high-fidelity AFM characterization and analysis. Meanwhile, the characterization data from AFM observation should be used in machine-learning models for a better understanding of the reaction mechanism.

ACKNOWLEDGMENTS

Manman Wang acknowledges support from the University of Surrey Vice-Chancellor's Studentship. Kai Yang and Yunlong Zhao acknowledge support from the EPSRC New Investigator Award (EP/V002260/1) and the Faraday Institution—Battery Study and Seed Research Project (FIRG052). Yundong Zhou thanks for the funding from Metrology and Standards for the Battery Value Chain of the National Measurement System of the UK Department of Business, Energy and Industrial Strategy.

CONFLICT OF INTEREST STATEMENT

The authors declare no conflict of interest.

ORCID

Kai Yang https://orcid.org/0000-0001-7391-1495

REFERENCES

- 1. He J, Lu C, Jiang H, et al. Scalable production of high-performing woven lithium-ion fibre batteries. *Nature*. 2021;597(7874):57-63.
- Li J, Fleetwood J, Hawley WB, Kays W. From materials to cell: state-of-the-art and prospective technologies for lithiumion battery electrode processing. *Chem Rev.* 2022;122(1): 903-956.
- Liu H, Zhu Z, Yan Q, et al. A disordered rock salt anode for fast-charging lithium-ion batteries. *Nature*. 2020;585(7823): 63-67.
- 4. Peters BK, Rodriguez KX, Reisberg SH, et al. Scalable and safe synthetic organic electroreduction inspired by Li-ion battery chemistry. *Science*. 2019;363(6429):838-845.
- Wang C-Y, Liu T, Yang X-G, et al. Fast charging of energydense lithium-ion batteries. *Nature*. 2022;611(7936):485-490.
- Winter M, Barnett B, Xu K. Before Li ion batteries. *Chem Rev.* 2018;118(23):11433-11456.
- Wu F, Maier J, Yu Y. Guidelines and trends for nextgeneration rechargeable lithium and lithium-ion batteries. Chem Soc Rev. 2020;49(5):1569-1614.
- 8. Asadi M, Sayahpour B, Abbasi P, et al. A lithium-oxygen battery with a long cycle life in an air-like atmosphere. *Nature*. 2018;555(7697):502-506.
- Chi X, Li M, Di J, et al. A highly stable and flexible zeolite electrolyte solid-state Li-air battery. *Nature*. 2021;592(7855): 551-557
- Liu T, Vivek JP, Zhao EW, Lei J, Garcia-Araez N, Grey CP. Current challenges and routes forward for nonaqueous lithium-air batteries. *Chem Rev.* 2020;120(14):6558-6625.
- Wu Z, Tian Y, Chen H, et al. Evolving aprotic Li–air batteries. Chem Soc Rev. 2022;51(18):8045-8101.
- Li Z, Sami I, Yang J, Li J, Kumar RV, Chhowalla M. Lithiated metallic molybdenum disulfide nanosheets for highperformance lithium-sulfur batteries. *Nat Energy*. 2023;8(1): 84-93
- Manthiram A, Fu Y, Chung S-H, Zu C, Su Y-S. Rechargeable Lithium–sulfur batteries. Chem Rev. 2014;114(23):11751-11787.
- Seh ZW, Sun Y, Zhang Q, Cui Y. Designing high-energy lithium-sulfur batteries. Chem Soc Rev. 2016;45(20):5605-5634.
- 15. Yang X, Luo J, Sun X. Towards high-performance solid-state Li–S batteries: from fundamental understanding to engineering design. *Chem Soc Rev.* 2020;49(7):2140-2195.
- 16. Pender JP, Jha G, Youn DH, et al. Electrode degradation in lithium-ion batteries. *ACS Nano*. 2020;14(2):1243-1295.
- 17. Zhang Z, Said S, Smith K, et al. Characterizing batteries by in situ electrochemical atomic force microscopy: a critical review. *Adv Energy Mater.* 2021;11(38):2101518.
- 18. Zhou Y, Su M, Yu X, et al. Real-time mass spectrometric characterization of the solid–electrolyte interphase of a lithium-ion battery. *Nat Nanotechnol.* 2020;15(3):224-230.

- 19. Li AL, Li G-H, Lu S-G, et al. Interface stabilization of 1,1,2,2-tetrafluoroethyl-2,2,3,3-tetrafluoropropyl ether to high-voltage Li-rich Mn-based layered cathode materials. *Rare Met.* 2022;41(3):822-829.
- 20. Kempaiah R, Vasudevamurthy G, Subramanian A. Scanning probe microscopy based characterization of battery materials, interfaces, and processes. *Nano Energy*. 2019;65:103925.
- 21. Wan J, Yan H-J, Wen R, Wan L-J. In situ visualization of electrochemical processes in solid-state lithium batteries. *ACS Energy Lett.* 2022;7(9):2988-3002.
- Wang S, Liu Q, Zhao C, et al. Advances in understanding materials for rechargeable lithium batteries by atomic force microscopy. Energy & Environmental Materials. 2018;1(1):28-40.
- Garcia R. Nanomechanical mapping of soft materials with the atomic force microscope: methods, theory and applications. *Chem Soc Rev.* 2020;49(16):5850-5884.
- 24. Heath GR, Kots E, Robertson JL, et al. Localization atomic force microscopy. *Nature*. 2021;594(7863):385-390.
- 25. Müller DJ, Dumitru AC, Lo Giudice C, et al. Atomic force microscopy-based force spectroscopy and multiparametric imaging of biomolecular and cellular systems. *Chem Rev.* 2021;121(19):11701-11725.
- 26. Zhang Z, Smith K, Jervis R, Shearing PR, Miller TS, Brett DJL. Operando electrochemical atomic force microscopy of solid–electrolyte interphase formation on graphite anodes: the evolution of SEI morphology and mechanical properties. ACS Appl Mater Interfaces. 2020;12(31):35132-35141.
- 27. Guo H-J, Sun Y, Zhao Y, et al. Surface degradation of single-crystalline Ni-rich cathode and regulation mechanism by atomic layer deposition in solid-state lithium batteries. *Angew Chem Int Ed.* 2022;61(48):e202211626.
- 28. Wang W-W, Gu Y, Yan H, et al. Evaluating solid-electrolyte interphases for lithium and lithium-free anodes from nanoindentation features. *Chem.* 2020;6(10):2728-2745.
- 29. McAllister QP, Strawhecker KE, Becker CR, Lundgren CA. In situ atomic force microscopy nanoindentation of lithiated silicon nanopillars for lithium ion batteries. *J Power Sources*. 2014;257:380-387.
- 30. Lang S-Y, Shi Y, Guo Y-G, Wen R, Wan L-J. Hightemperature formation of a functional film at the cathode/ electrolyte interface in lithium-sulfur batteries: an in situ AFM study. *Angew Chem Int Ed.* 2017;56(46):14433-14437.
- Wen R, Hong M, Byon HR. In situ AFM imaging of Li-O₂ electrochemical reaction on highly oriented pyrolytic graphite with ether-based electrolyte. *J Am Chem Soc.* 2013;135(29):10870-10876.
- 32. Hu J, Li L, Hu E, et al. Mesoscale-architecture-based crack evolution dictating cycling stability of advanced lithium ion batteries. *Nano Energy*. 2021;79:105420.
- 33. Yang K, Jia L, Liu X, et al. Revealing the anion intercalation behavior and surface evolution of graphite in dual-ion batteries via in situ AFM. *Nano Res.* 2020;13(2):412-418.
- Kim K, Hwang D, Kim S, et al. Cyclic aminosilane-based additive ensuring stable electrode–electrolyte interfaces in Liion batteries. Adv Energy Mater. 2020;10(15):2000012.
- Yu X, Manthiram A. Electrode–electrolyte interfaces in lithium-based batteries. *Energy Environ Sci.* 2018;11(3): 527-543.

- Takenaka N, Bouibes A, Yamada Y, Nagaoka M, Yamada A. Frontiers in theoretical analysis of solid electrolyte interphase formation mechanism. *Adv Mater*. 2021;33(37):2100574.
- 37. Han W-W, Ardhi REA, Liu G-C. Dual impact of superior SEI and separator wettability to inhibit lithium dendrite growth. *Rare Met.* 2022;41(2):353-355.
- 38. Haruta M, Kijima Y, Hioki R, Doi T, Inaba M. Artificial lithium fluoride surface coating on silicon negative electrodes for the inhibition of electrolyte decomposition in lithiumion batteries: visualization of a solid electrolyte interphase using in situ AFM. *Nanoscale*. 2018;10(36):17257-17264.
- 39. Tokranov A, Sheldon BW, Li C, Minne S, Xiao X. In situ atomic force microscopy study of initial solid electrolyte interphase formation on silicon electrodes for Li-ion batteries. *ACS Appl Mater Interfaces*. 2014;6(9):6672-6686.
- Cresce A, Russell SM, Baker DR, Gaskell KJ, Xu K. In situ and quantitative characterization of solid electrolyte interphases. *Nano Lett.* 2014;14(3):1405-1412.
- 41. Lin L, Yang K, Tan R, et al. Effect of sulfur-containing additives on the formation of a solid-electrolyte interphase evaluated by in situ AFM and ex situ characterizations. *J Mater Chem A*. 2017;5(36):19364-19370.
- 42. Liu T, Lin L, Bi X, et al. In situ quantification of interphasial chemistry in Li-ion battery. *Nat Nanotechnol.* 2019;14(1): 50-56.
- 43. Yu H, Zhao J, Ben L, Zhan Y, Wu Y, Huang X. Dendrite-free lithium deposition with self-aligned columnar structure in a carbonate–ether mixed electrolyte. *ACS Energy Lett.* 2017; 2(6):1296-1302.
- Zhao C-Z, Cheng X-B, Zhang R, et al. Li₂S₅-based ternary-salt electrolyte for robust lithium metal anode. *Energy Storage Mater*. 2016;3:77-84.
- 45. Liu X-R, Wang L, Wan L-J, Wang D. In situ observation of electrolyte-concentration-dependent solid electrolyte interphase on graphite in dimethyl sulfoxide. *ACS Appl Mater Interfaces*. 2015;7(18):9573-9580.
- 46. Shen C, Wang S, Jin Y, Han W-Q. In situ AFM imaging of solid electrolyte interfaces on HOPG with ethylene carbonate and fluoroethylene carbonate-based electrolytes. ACS Appl Mater Interfaces. 2015;7(45):25441-25447.
- 47. Wang M, Huai L, Hu G, et al. Effect of LiFSI concentrations to form thickness- and modulus-controlled SEI layers on lithium metal anodes. *J Phys Chem C*. 2018;122(18): 9825-9834.
- 48. Fedorov MV, Kornyshev AA. Ionic liquids at electrified interfaces. *Chem Rev.* 2014;114(5):2978-3036.
- 49. Hayes R, Warr GG, Atkin R. Structure and nanostructure in ionic liquids. *Chem Rev.* 2015;115(13):6357-6426.
- Shi Y, Yan H-J, Wen R, Wan L-J. Direct visualization of nucleation and growth processes of solid electrolyte interphase film using in situ atomic force microscopy. ACS Appl Mater Interfaces. 2017;9(26):22063-22067.
- 51. Li G, Gao Y, He X, et al. Organosulfide-plasticized solidelectrolyte interphase layer enables stable lithium metal anodes for long-cycle lithium-sulfur batteries. *Nat Commun*. 2017;8(1):850.
- 52. Zhao Y, Li G, Gao Y, Wang D, Huang Q, Wang D. Stable Li metal anode by a hybrid lithium polysulfidophosphate/

- polymer cross-linking film. ACS Energy Lett. 2019;4(6): 1271-1278.
- Zampardi G, Klink S, Kuznetsov V, et al. Combined AFM/ SECM investigation of the solid electrolyte interphase in Liion batteries. *ChemElectroChem.* 2015;2(10):1607-1611.
- 54. Steinhauer M, Stich M, Kurniawan M, et al. In situ studies of solid electrolyte interphase (SEI) formation on crystalline carbon surfaces by neutron reflectometry and atomic force microscopy. *ACS Appl Mater Interfaces*. 2017;9(41):35794-35801.
- 55. Li S, Wang C, Meng C, Ning Y, Zhang G, Fu Q. Electrolyte-dependent formation of solid electrolyte interphase and ion intercalation revealed by in situ surface characterizations. *J Energy Chem.* 2022;67:718-726.
- Cheng H, Shapter JG, Li Y, Gao G. Recent progress of advanced anode materials of lithium-ion batteries. *J Energy Chem.* 2021;57:451-468.
- 57. Lu J, Chen Z, Pan F, Cui Y, Amine K. High-performance anode materials for rechargeable Lithium-ion batteries. *Electrochem Energy Rev.* 2018;1(1):35-53.
- 58. Nzereogu PU, Omah AD, Ezema FI, Iwuoha EI, Nwanya AC. Anode materials for lithium-ion batteries: a review. *Appl Surf Sci Adv.* 2022;9:100233.
- Reddy MV, Subba Rao GV, Chowdari BVR. Metal oxides and oxysalts as anode materials for Li ion batteries. *Chem Rev.* 2013;113(7):5364-5457.
- Zhao R, Wang S, Liu D, et al. Effect of fluoroethylene carbonate on solid electrolyte interphase formation of the SiO/C anode observed by in situ atomic force microscopy. ACS Appl Energy Mater. 2021;4(1):492-499.
- Jiang Z, Guo H-J, Zeng Z, et al. In situ characterization of over-lithiation of organosulfide-based lithium metal anodes. ACS Appl Mater Interfaces. 2021;13(35):41555-41562.
- Lucas IT, Pollak E, Kostecki R. In situ AFM studies of SEI formation at a Sn electrode. *Electrochem Commun.* 2009;11(11): 2157-2160.
- 63. Wang S, Yang K, Gao F, Wang D, Shen C. Direct visualization of solid electrolyte interphase on $\text{Li}_4\text{Ti}_5\text{O}_{12}$ by in situ AFM. RSC Adv. 2016;6(81):77105-77110.
- 64. Wang S, Zhang W, Chen Y, et al. Operando study of Fe₃O₄ anodes by electrochemical atomic force microscopy. *Appl Surf Sci.* 2017;426:217-223.
- 65. Sungjemmenla, SKV, Soni CB, Kumar V, Seh ZW. Understanding the cathode–electrolyte interphase in lithium-ion batteries. *Energy Technol.* 2022;10(9):2200421.
- 66. Lu W, Zhang J, Xu J, Wu X, Chen L. In situ visualized cathode electrolyte interphase on LiCoO₂ in high voltage cycling. *ACS Appl Mater Interfaces*. 2017;9(22):19313-19318.
- 67. Liu R-R, Deng X, Liu X-R, Yan H-J, Cao A-M, Wang D. Facet dependent SEI formation on the LiNi $_{0.5}$ Mn $_{1.5}$ O $_4$ cathode identified by in situ single particle atomic force microscopy. *Chem Commun.* 2014;50(99):15756-15759.
- 68. Chen M, Wang W, Shi Z, Liu Z, Shen C. Revealing the cathode electrolyte interphase on Li- and Mn-rich materials by in-situ electrochemical atomic force microscopy. *Appl Surf Sci.* 2022;600:154119.
- 69. Stallard JC, Wheatcroft L, Booth SG, et al. Mechanical properties of cathode materials for lithium-ion batteries. *Joule.* 2022;6(5):984-1007.

- Tokranov A, Kumar R, Li C, Minne S, Xiao X, Sheldon BW. Control and optimization of the electrochemical and mechanical properties of the solid electrolyte interphase on silicon electrodes in lithium ion batteries. *Adv Energy Mater*. 2016;6(8):1502302.
- 71. Li P, Kang Z, Zhang Z, et al. In situ microscopy techniques for characterizing the mechanical properties and deformation behavior of two-dimensional (2D) materials. *Mater Today*. 2021;51:247-272.
- 72. Li X, Sun M, Shan C, Chen Q, Wei X. Mechanical properties of 2D materials studied by in situ microscopy techniques. *Adv Mater Interfaces*. 2018;5(5):1701246.
- 73. Fu Y, Yang K, Xue S, et al. Surface defects reinforced polymer-ceramic interfacial anchoring for high-rate flexible solid-state batteries. *Adv Funct Mater.* 2023;33(10):2210845.
- Ji Y, Yang K, Liu M, et al. PIM-1 as a multifunctional framework to enable high-performance solid-state lithium-sulfur batteries. *Adv Funct Mater.* 2021;31(47):2104830.
- Liu X-R, Deng X, Liu R-R, et al. Single nanowire electrode electrochemistry of silicon anode by in situ atomic force microscopy: solid electrolyte interphase growth and mechanical properties. ACS Appl Mater Interfaces. 2014;6(22): 20317-20323.
- Guo H-J, Wang H-X, Guo Y-J, et al. Dynamic evolution of a cathode interphase layer at the surface of LiNi_{0.5}Co_{0.2}Mn_{0.3}O₂ in quasi-solid-state lithium batteries. *J Am Chem Soc.* 2020; 142(49):20752-20762.
- 77. Tan DHS, Chen Y-T, Yang H, et al. Carbon-free high-loading silicon anodes enabled by sulfide solid electrolytes. *Science*. 2021;373(6562):1494-1499.
- Ko M, Chae S, Ma J, et al. Scalable synthesis of siliconnanolayer-embedded graphite for high-energy lithium-ion batteries. *Nat Energy*. 2016;1(9):16113.
- Liu Q, Hu Y, Yu X, Qin Y, Meng T, Hu X. The pursuit of commercial silicon-based microparticle anodes for advanced lithium-ion batteries: a review. *Nano Res Energy*. 2022; 1:e9120037.
- Song Z, Wang L, Yang K, et al. Intermolecular chemistry for designing functional binders in silicon/carbon composite anodes. *Mater Today Energy*. 2022;30:101153.
- 81. Liu J, Lee SY, Yoo J, Kim S, Kim J-H, Cho H. Real-time observation of mechanical evolution of micro-sized Si anodes by in situ atomic force microscopy. *ACS Mater Letters*. 2022;4(5):840-846.
- 82. Boebinger MG, Yarema O, Yarema M, et al. Spontaneous and reversible hollowing of alloy anode nanocrystals for stable battery cycling. *Nat Nanotechnol.* 2020;15(6):475-481.
- Chen J, Fan X, Li Q, et al. Electrolyte design for LiF-rich solid–electrolyte interfaces to enable high-performance microsized alloy anodes for batteries. *Nat Energy*. 2020;5(5):386-397.
- 84. Li H, Yamaguchi T, Matsumoto S, et al. Circumventing huge volume strain in alloy anodes of lithium batteries. *Nat Commun.* 2020;11(1):1584.
- 85. Lu Y, Zhao C-Z, Zhang R, et al. The carrier transition from Li atoms to Li vacancies in solid-state lithium alloy anodes. *Sci Adv.* 2021;7(38):eabi5520.
- 86. Wang H, Wang C, Tang Y. Interface engineering toward high-efficiency alloy anode for next-generation energy storage device. *EcoMat.* 2021;3(6):e12172.

- 87. Becker CR, Strawhecker KE, McAllister QP, Lundgren CA. In situ atomic force microscopy of lithiation and delithiation of silicon nanostructures for lithium ion batteries. *ACS Nano*. 2013;7(10):9173-9182.
- 88. Kumar R, Tokranov A, Sheldon BW, et al. In situ and operando investigations of failure mechanisms of the solid electrolyte interphase on silicon electrodes. *ACS Energy Lett.* 2016;1(4):689-697.
- 89. Wan J, Hao Y, Shi Y, et al. Ultra-thin solid electrolyte interphase evolution and wrinkling processes in molybdenum disulfide-based lithium-ion batteries. *Nat Commun.* 2019:10(1):3265.
- 90. Wan J, Song Y-X, Chen W-P, et al. Micromechanism in all-solid-state alloy-metal batteries: regulating homogeneous lithium precipitation and flexible solid electrolyte interphase evolution. *J Am Chem Soc.* 2021;143(2):839-848.
- 91. Jie Y, Xu Y, Chen Y, et al. Molecular understanding of interphase formation via operando polymerization on lithium metal anode. *Cell Rep Phys Sci.* 2022;3(10):101057.
- 92. Li N-W, Shi Y, Yin Y-X, et al. A flexible solid electrolyte interphase layer for long-life lithium metal anodes. *Angew Chem Int Ed.* 2018;57(6):1505-1509.
- 93. Wan J, Chen W-P, Liu G-X, et al. Insights into the nitride-regulated processes at the electrolyte/electrode interface in quasi-solid-state lithium metal batteries. *J Energy Chem.* 2022;67:780-786.
- Wang S, Liu D, Cai X, et al. Promoting the reversibility of lithium ion/lithium metal hybrid graphite anode by regulating solid electrolyte interface. *Nano Energy*. 2021;90:106510.
- 95. Lang S-Y, Xiao R-J, Gu L, Guo Y-G, Wen R, Wan L-J. Interfacial mechanism in lithium–sulfur batteries: how salts mediate the structure evolution and dynamics. *J Am Chem Soc.* 2018;140(26):8147-8155.
- Liu G-X, Wan J, Shi Y, et al. Direct tracking of additiveregulated evolution on the lithium anode in quasi-solid-state lithium-sulfur batteries. Adv Energy Mater. 2022;12(40): 2201411.
- 97. Mahankali K, Thangavel NK, Reddy Arava LM. In situ electrochemical mapping of lithium–sulfur battery interfaces using AFM–SECM. *Nano Lett.* 2019;19(8):5229-5236.
- 98. Song Y-X, Wan J, Guo H-J, et al. Insights into evolution processes and degradation mechanisms of anion-tunable interfacial stability in all-solid-state lithium-sulfur batteries. *Energy Storage Mater.* 2021;41:642-649.
- 99. Shen Z-Z, Lang S-Y, Shi Y, Ma J-M, Wen R, Wan L-J. Revealing the surface effect of the soluble catalyst on oxygen reduction/evolution in Li-O₂ batteries. *J Am Chem Soc.* 2019;141(17):6900-6905.
- 100. Shen Z-Z, Zhang Y-Z, Zhou C, Wen R, Wan L-J. Revealing the correlations between morphological evolution and surface reactivity of catalytic cathodes in lithium–oxygen batteries. *J Am Chem Soc.* 2021;143(51):21604-21612.
- 101. Shen Z-Z, Zhou C, Wen R, Wan L-J. Surface mechanism of catalytic electrodes in lithium-oxygen batteries: how nanostructures mediate the interfacial reactions. *J Am Chem Soc.* 2020;142(37):16007-16015.
- 102. Wen R, Byon HR. In situ monitoring of the Li-O₂ electrochemical reaction on nanoporous gold using

- electrochemical AFM. *Chem Commun.* 2014;50(20): 2628-2631.
- 103. Shen C, Hu G, Cheong L-Z, Huang S, Zhang J-G, Wang D. Direct observation of the growth of lithium dendrites on graphite anodes by operando EC-AFM. Small Methods. 2018;2(2):1700298.
- 104. Alikin DO, Romanyuk KN, Slautin BN, Rosato D, Shur VY, Kholkin AL. Quantitative characterization of the ionic mobility and concentration in Li-battery cathodes via low frequency electrochemical strain microscopy. *Nanoscale*. 2018;10(5):2503-2511.
- 105. Yang S, Yan B, Wu J, Lu L, Zeng K. Temperature-dependent lithium-ion diffusion and activation energy of Li_{1.2}Co_{0.13} Ni_{0.13}Mn_{0.54}O₂ thin-film cathode at nanoscale by using electrochemical strain microscopy. ACS Appl Mater Interfaces. 2017;9(16):13999-14005.
- 106. Zhu J, Lu L, Zeng K. Nanoscale mapping of lithium-ion diffusion in a cathode within an all-solid-state lithium-ion battery by advanced scanning probe microscopy techniques. ACS Nano. 2013;7(2):1666-1675.
- Lipson AL, Ginder RS, Hersam MC. Nanoscale in situ characterization of L-ion battery electrochemistry via scanning ion conductance microscopy. *Adv Mater*. 2011;23(47): 5613-5617.
- 108. Payne NA, Dawkins JIG, Schougaard SB, Mauzeroll J. Effect of substrate permeability on scanning ion conductance microscopy: uncertainty in tip-substrate separation and determination of ionic conductivity. *Anal Chem.* 2019;91(24): 15718-15725.
- 109. Masuda H, Ishida N, Ogata Y, Ito D, Fujita D. Internal potential mapping of charged solid-state-lithium ion batteries using in situ Kelvin probe force microscopy. *Nanoscale*. 2017;9(2):893-898.
- Masuda H, Matsushita K, Ito D, Fujita D, Ishida N. Dynamically visualizing battery reactions by operando Kelvin probe force microscopy. *Commun Chem.* 2019;2(1):140.
- 111. Zhu X, Revilla RI, Hubin A. Direct correlation between local surface potential measured by Kelvin probe force microscope and electrochemical potential of LiNi_{0.80}Co_{0.15}Al_{0.05}O₂ cathode at different state of charge. *J Phys Chem C*. 2018;122(50): 28556-28563.

AUTHOR BIOGRAPHIES



Dr Yundong Zhou is a higher scientist at the National Physical Laboratory (UK). He received a PhD degree from the Institute for Frontier Materials, Deakin University. He did research in polymer/ionic liquid and ceramic solid-

state batteries and in situ Raman for solid-state batteries. Then, he joined the National Centre of Excellence for Mass Spectrometry Imaging at NPL to develop the technique TOF-SIMS (high spatial resolution) and OrbiSIMS (high mass resolution) for

studying material surfaces and interfaces, especially on battery SEI and degradation mechanism, and perovskite solar cells, semiconductors, core-shell particles, and 3D printing devices.



Dr Yunlong Zhao is an associate professor at the Dyson School of Design Engineering, Imperial College London. He also holds a joint appointment at the National Physical Laboratory (UK) as a senior scientist. Dr

Yunlong Zhao has developed a series of novel electrochemical energy devices, sensors, and their integration into 2D on-chip and 3D soft systems for in-depth studies of electrochemistry, electrophysiology, and healthcare, with over 90 publications and 9000 citations. His research interests include advanced electrochemical energy storage devices, bioelectronic devices/sensors, and integrated on-chip and 3D soft electronic systems.



Dr Kai Yang is a lecturer in the Advanced Technology Institute at the University of Surrey. He received his PhD degree from the School of Advanced Materials at Peking University Shenzhen Graduate School in Prof. Feng Pan's group. His research

interests mainly focus on developing in situ characterizations for interfacial research in energy storage/conversion material and devices, developing composite solid electrolytes for SSBs, carbon dioxide fixation and utilization technologies such as Li/Na/Zn-CO₂ battery, and developing nanoelectronics platforms for energy applications.

How to cite this article: Wang M, Song Z, Bi J, et al. Probing interfacial electrochemistry by in situ atomic force microscope for battery characterization. *Battery Energy.* 2023;2:2023006. doi:10.1002/bte2.2023006